Ampoule and Nozzle Development for Needle-Free Injections

John Liu, N. Catherine Hogan, and Ian Hunter, *Member, IEEE*

***Abstract*—A rigid, compact, multi-piece ampoule has been designed and fabricated as a platform to conveniently house different nozzle inserts one at a time to offer increased jet consistency and functional flexibility. Three different nozzle geometries that respectively produce a single axial jet, radial jets, and intersecting jets are designed and fabricated. Through high-speed imaging and injection into tissue analog and *ex vivo* porcine tissue, these nozzles are demonstrated to have potential for a range of injection applications including intradermal, intratympanic, and traditional uses. The presented ampoule is more successful than a commercial jet injection ampoule in adhering to desired position and velocity trajectories and the energy efficiencies of jet ejections are compared.**

I. Introduction

The development of needle-free injection (NFI) systems has become increasingly important because of the advantages it affords such as increased patient acceptability, enhanced occupational safety for health providers, safe disposal, and increased speed of mass vaccination in the face of pandemic influenza or bioterror emergencies. Jet injection, wherein drug is propelled at high pressure through a narrow orifice to create a high-speed fluid jet sufficient to penetrate tissue, is one of several needle-free methods for administration of drug [1].

While actuator and controller designs advance [2-5], ampoule and nozzle designs have remained static and options are limited to two groups: commercial jet injection ampoules and industrial-grade nozzles incorporated into machined ampoules. Mainstream commercial jet injectors such as Bioject®, Vitajet®, or Injex® utilize injection molding to manufacture nozzles [6]. However, the manufacturing tolerances for these nozzles are not sufficient for the purpose of controlled fluid experiments. Even when two nozzles are of comparable diameters, the three-dimensional morphology of the interior can differ significantly from nozzle to nozzle. Such variation can alter the ejected jet shape and consequently the depth and dispersion of the fluid jet in tissue as shown by [7]. In addition to manufacturing variability in nozzle geometry, injection-molded nozzles also deform over the course of repeated injections, due to the high pressure the nozzle is subject to during injection. Finally, the compliance of some commercial pistons causes ringing during injection, which decreases control over both the jet velocity and volume [8]. To counter some of the above issues, some research groups employ jeweled orifices [9] or ceramic nozzles [10-11] that are incorporated into custom-made ampoules. While the geometry of such orifices are manufactured to micron tolerances and do not deform over the course of repeated experiments, nozzle geometries are limited and only produce single axial jets.

In this paper, we discuss the development of an ampoule that offers increased jet consistency and functional flexibility. A rigid, compact, multi-piece ampoule has been designed and fabricated as a platform to conveniently house different nozzle inserts, one at a time. Three different nozzle geometries that respectively produce a single axial jet, radial jets, and intersecting jets are designed, fabricated, demonstrated, and compared to a commercial JI ampoule.

II. Device Design and Manufacturing

A. Ampoule Design and Machining

The multi-piece ampoule system (Fig. 1a) consists of four parts: 1) a body in which the drug is stored, 2) a piston that travels through the entirety of the ampoule body, 3) a nozzle insert, and 4) a hex head that attaches to the threads of the ampoule to create the necessary force against the O-ring to create a fluidic seal between the nozzle insert and ampoule body. The ampoule body, head, and nozzle are composed of 303 stainless steel, whereas the piston is machined out of W1 tool steel (cross section shown in Fig. 1a right inset).

The ampoule body is 40 mm long and has an inner diameter of 3.53 mm with a volume drug capacity of over 350 μL. The exterior features of the body are machined using a CNC lathe, and the body's cavity is machined via three steps: drilling, reaming, and three stages of honing (120, 340, and 600 grit). This yields a polished surface finish to enable the fluidic seal required between the piston and interior of the ampoule body. The interior of the hex head has inner threads 6.5 mm long that end with an inner relief of 1 mm—this means that the ampoule can easily host nozzle inserts of 1 to 5 mm in axial length, and lengths less than 1 mm if a spacer is placed between the nozzle insert and inner face of the ampoule hex head.

The piston composed of W1 tool steel has two Buna-N O-rings (durometer rating of 70A) that sit behind the head in grooves—the first O-ring serves as the primary fluidic seal while the second enables the piston's alignment to the axis of the ampoule body. Because the tip of the presented piston is rigid and cannot be deformed as can some of the commercial piston tips (e.g. Injex) the tip geometry was designed to match the interior geometry of the nozzle, to avoid introducing a bubble into the ampoule when drug is drawn into the ampoule. In this presentation (Fig. 1a left inset) the piston tip was designed to match the interior of the Injex nozzle.

J. Liu is with the Department of Mechanical Engineering, Massachusetts Institute of Technology, Room 3-147, 77 Massachusetts Ave, Cambridge, MA 02139, USA (phone: 617-258-0533 email: johnhliu@mit.edu).

N. C. Hogan is a Research Scientist with the BioInstrumentation Lab, Massachusetts Institute of Technology (email:hog@mit.edu)
I. W. Hunter is a Professor of the Department of Mechanical Engineering, Massachusetts Institute of Technology (email:ihunter@mit.edu)

978-1-5090-2809-2/17/$31.00 ©2017 IEEE

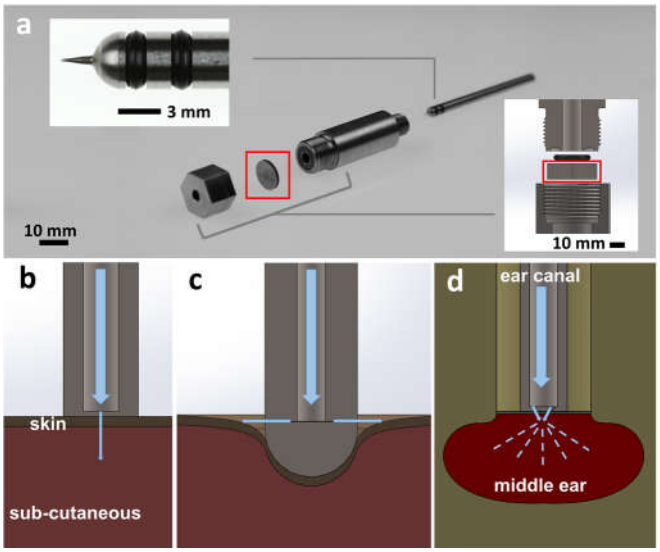

Figure 1. The multi-piece ampoule. (a) A picture showing the four parts (left to right): head, nozzle insert (boxed in red), body, and piston with a close-up of its tip (left inset). A cross section (right inset) shows the ampoule body seats an O-ring in a circular groove, a nozzle insert (boxed in red) that is readily exchanged, and a head that attaches to the threads of the ampoule body and compresses the O-ring to form the fluidic seal. Three nozzles inserts are designed and fabricated to be housed in the ampoule one at a time: (b) the standard nozzle that produces a single jet along the axis of the ampoule for traditional NFI injections, (c) the radial jets nozzle for intradermal injection, and (d) the intersecting jets nozzle for intratympanic injection. (Blue arrows indicate direction of fluid flow, dotted blue signifies dispersed fluid.)

B. Nozzle Geometry Function, Design, and Manufacturing

Three nozzles are designed and fabricated: the standard nozzle, the radial jets nozzle, and the intersecting jets nozzle. Because of the multi-piece ampoule design, each of these nozzles of different overall geometries are readily housed in the multi-piece ampoule without any additional adjustment.

The standard nozzle produces a single jet along the axis of the ampoule providing a standard of comparison to most commercially available nozzles (including the Injex) (Fig. 1b). 0.5 to 1 mm thickness disks of 303 stainless steel were cut using a wire electrical discharge machine (wire EDM). The surfaces were polished either using a grinding wheel or finishing passes on the wire EDM. The orifice is created using a 200 µm diameter micro-drill and standard drill press (Servo®, Model 1760).

The radial jets nozzle diagrammed in Fig. 1c is designed specifically for intradermal injection. Dermal therapeutics that may benefit from intradermal NFI include vaccine, anesthetic, and dermal filler delivery. Jets for intradermal injections must fulfill two conditions: 1) cause the drug to breach the dermis but 2) avoid depositing the bulk of the drug beyond the dermis. Because the human dermis ranges from 2 – 3.5 mm in thickness and the epidermal toughness ranges from location to location, the range of velocity profiles for traditional axial jets that will achieve both conditions is both tight and highly variable between site to site and person to person. The radial jets nozzle is machined out of carbon steel on a CNC lathe. The head is 5 mm in diameter and has the end of a sphere to match the profile of the skin when indented by the nozzle. Two orifices are created using a 150 µm diameter micro-drill on opposing sides of the nozzle right above the sphere end. When the nozzle is indented into the skin, the exiting jets are aligned with the plane of the skin. Thus, as long as the dermis is breached, a jet will generally remain traveling in the dermis regardless of a lower or higher velocity.

The intersecting jets nozzle is purposed for the general class of NFI applications where there exist areas beyond a certain distance that will be damaged by a high velocity jet or a fixed depth is otherwise a high priority. In intratympanic injections, for example, an NFI jet must breach the tympanic membrane then suddenly lose the bulk of its axial momentum to prevent damaging sensitive components that lay just beyond the membrane in the middle ear, such as the auditory ossicles. The presented nozzle (Fig. 1d) offers the potential to actualize tympanic NFI by shooting jets to breach the tympanic membrane, then intersecting with each other, thereby losing much of its kinetic energy. Intersecting jets has found application in debridement [11] but to the authors' knowledge, no such development exists for NFI application.

The intersecting jets nozzle is machined out of 303 stainless steel on a CNC lathe. The head is composed of a long and slender column 4 mm in diameter to travel through the ear canal until the nozzle face rests against the tympanic membrane. Two orifices 1.73 mm apart at 30 degree angles with respect to the ampoule axis are created using a 200 µm diameter micro-drill, producing two jets that intersect ~1.5 mm from the exit. Because micro-drills will slip and eventually break if used to drill at a significant angle, a shallow 2 mm diameter conical recess is first machined, yielding an incline that presents a perpendicular surface for angled micro-drilling.

III. Materials and Methods

A. Jet Injector System

Experimentation was performed using the controllable Lorentz-force actuated jet injection device developed in the MIT BioInstrumentation Lab [3]. The position control of the coil is achieved using a compact reconfigurable system consisting of a real-time controller (cRIO-9004, National Instruments, Austin, TX) embedded in a reconfigurable field-programmable gate-array (FPGA) chassis (cRIO-9113) as detailed in [3].

B. High-speed Imaging

The ejections of fluid jets into air and injections into acrylamide gel were recorded by a high-speed CMOS video camera (Vision Research®, Phantom V9) fitted with a 50 mm compact macro lens (Canon Compact Macro-Lens EF) at frame rates of 2000 to 6400 fps with exposure times of 155 to 500 µs. Lighting was provided by an arrangement of halogen LED lamps.

C. Injections

For injections into tissue analog, acrylamide gel, gel (10%) was prepared as described in [12] and injection into gels was visualized using 1:100 dilution of blue tissue marking dye (Polysciences®). After injection, the acrylamide gels were photographed on a lightbox using a Canon 7D camera with a 100 mm compact macron lens (Canon Compact Macro-Lens EF). The same velocity profile was used across all acrylamide injections: jet velocity (v_{jet}) of 100 m/s, time at v_{jet} (t_{jet}) of 2 ms, follow through velocity (v_{ft}) of 50 m/s, with a volume per injection of 50 µL.

Two types of injections were additionally carried out to demonstrate the function of a radial jets nozzle and intersecting jets nozzle. For the radial jets nozzle, injections into *ex vivo* porcine abdominal tissue were carried out. For the intersecting jets nozzle, injections into *ex vivo* porcine tissue and tympanic membrane analog were done.

Post-mortem tissue was obtained through the MIT Tissue Harvest Program using procedures approved by the IUCAC and in accordance with the NIH Guide for the Use and Care of Laboratory Animals. Tissue was harvested from the abdomen of Yorkshire pigs (approximately 6 months) immediately after euthanasia and included skin and underlying subcutis and muscle. The tissue was trimmed, immediately vacuum sealed, and stored at -80°C. Prior to injection, each sample was thawed at 4°C and equilibrated to room temperature. The radial jets nozzle was placed in direct contact with the tissue and pressed in such a way that the bottom edge of the ampoule hex lightly contacts the skin. Porcine tissue samples were injected with tissue marking dye (as above), using a v_{jet} of 160 m/s, t_{jet} of 2 ms, v_{ft} of 50 m/s, and volume of 50 µL, after which the tissue was frozen, medially sectioned, splayed injection side up, and photographed using a Canon 1D camera and 100 mm lens.

Tympanic membrane analog injections were set up by fixing a tympanic membrane analog over a vial of acrylamide gel (10%) in which the surface of the gel was more than 2 mm below the top lip of the vial—the gel represents the sensitive auditory components beyond the tympanic membrane. A tympanic membrane analog was composed by fixing silicone rubber onto porous paper, yielding a sheet of ~0.13 mm thickness. The face of the intersecting jets nozzle was placed in direct contact with the membrane. After injection, the acrylamide gel was photographed in the same way as described above for acrylamide injections.

D. Ejection Efficiency

The ejection efficiency is calculated as a ratio of the mechanical kinetic energy of the exiting jet over the electrical energy input to the coil of the Lorentz-force actuator. The electrical energy input is calculated by performing a discrete time integration of the product between the current and voltage profiles,

$$E_{in} = E_{electrical} = \sum_i P(i)V(i)\Delta t, \quad (1)$$

where P is power, V is voltage, and Δt is the time step.

To calculate the mechanical kinetic energy of the jet, the inlet velocity is first calculated by taking the discrete derivative of the position profile of the piston, then smoothed using a third order Savitzky-Golay filter. The outlet velocity, v_{outlet}, is then calculated using conservation of mass, in which the velocity profile of the jet across the diameter of the orifice has been approximated as uniform,

$$v_{outlet}(i) = \frac{A_{inlet}}{A_{outlet}} \frac{x(i)-x(i-1)}{\Delta t}, \quad (2)$$

where A_{inlet} and A_{outlet} are areas of the inlet and outlet, respectively, and x is the position of the piston. The mechanical energy output is then calculated as the discrete time integration of the product between dynamic pressure and flow rate,

$$E_{out} = E_{kinetic} = \sum_i \left(\frac{1}{2}\rho v_{outlet}(i)^2\right)\left(\pi r^2 v_{outlet}(i)\right)\Delta t, \quad (3)$$

where ρ is the fluid density and r is the orifice radius.

In all numerical integrations, Δt is 10 µs. Ten ejection trials were performed using the same velocity profile (v_{jet} of 100 m/s, t_{jet} of 2 ms, v_{ft} of 50 m/s, and volume of 50 µL) to obtain the average efficiency and standard deviation. Nozzle radii were measured using a scanning electron microscope (SEM, TM3000 Hitachi).

IV. Results and Discussion

A. Piston Trajectory

Fig. 2 compares the performances of the Injex ampoule and multi-piece ampoule in a side-by-side plot comparison of representative trajectories of exit velocity of the fluid (Fig. 2a-b) and piston position (Fig. 2c-d) over time. In both cases, there are two instances of significant deviation from the desired exit velocity. The first is the spike up in velocity at the beginning of the v_{jet} phase and the second is the spike down in the transition at the end of the v_{jet} phase. The velocity spikes due to the rigid piston's travel in the multi-piece ampoule are significantly smaller in the case of the multi-piece ampoule—~80% and ~65% less than those observed of the original velocity spikes in the Injex configuration. A significant decrease in ringing during the v_{jet} phase of the ejection using the multi-piece ampoule is also observed. The presented system significantly improves the adherence of the actual velocity trajectories to the desired trajectories.

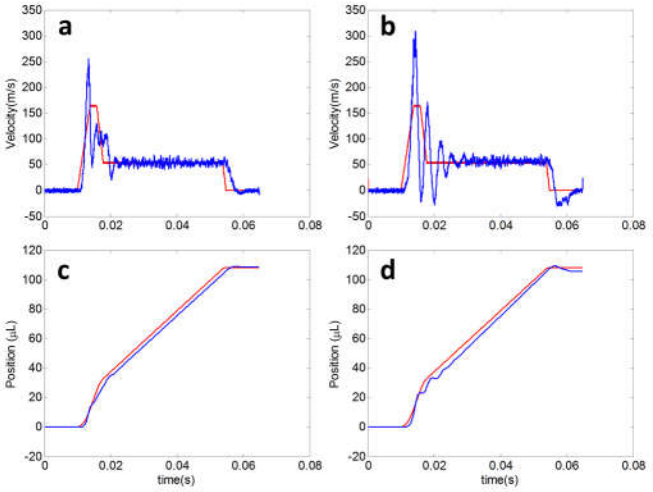

Figure 2. Representative plots of actual (**blue**) and desired (**red**) velocity and position trajectories of the multi-piece ampoule and Injex ampoule during jet ejection (v_{jet} of 160 m/s, t_{jet} of 2 ms, v_{ft} of 50 m/s volume of 110 µL). Fluid velocity trajectories of the (a) multi-piece ampoule and (b) Injex ampoule and piston position (volume) trajectories of the (c) multi-piece ampoule and (d) Injex ampoule.

B. Jet Ejections

High speed imaging shows that jets ejected from the standard nozzle, radial jets nozzle, and intersecting jets are well collimated and not dispersed (Fig. 3a-c). Unlike the often-observed defects in Injex ampoules introduced by commercial injection molding [7], the cylindrical orifices produced by micro-drilling do not generally have significant burrs or internal obstructions to flow and thus the manufacturing of the

presented nozzles consistently yield nozzles that produce collimated jets. In the ejected jets from the intersecting jets nozzle, significant dispersion and fluid atomization is observed ~1.5 mm downstream. Because these nozzle inserts are machined out of stainless steel or carbon steel, the interior geometry will not deform over time and is therefore suitable for controlled experiments over many trials.

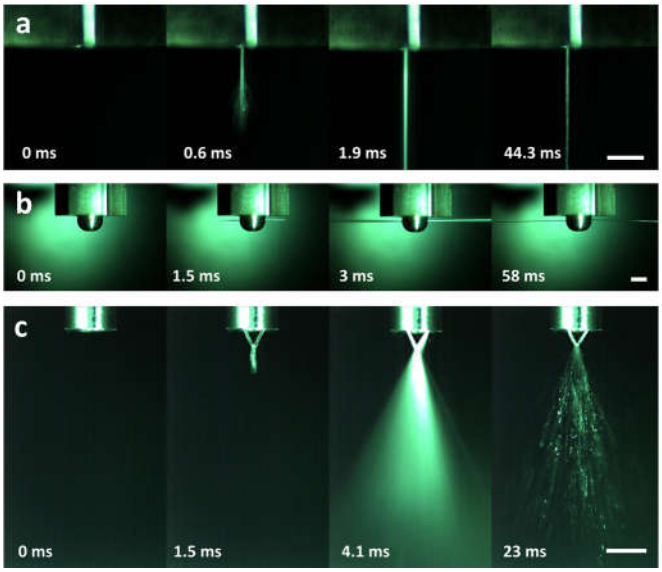

Figure 3. High-speed images of ejected jets of the (a) standard nozzle (6400 fps), (b) radial jets nozzle (2000 fps), and (c) intersecting jets nozzle (4000 fps). (Scale bar = 3 mm.)

C. *Standard Nozzle*

Injection into acrylamide gel and *ex vivo* porcine tissue via a jet from a standard nozzle yields the commonly-observed channel and bolus (Fig. 4a, 4c) [13], similar to the injection shape caused by a jet from the Injex ampoule using the same injection parameters (Fig. 4b, 4d).

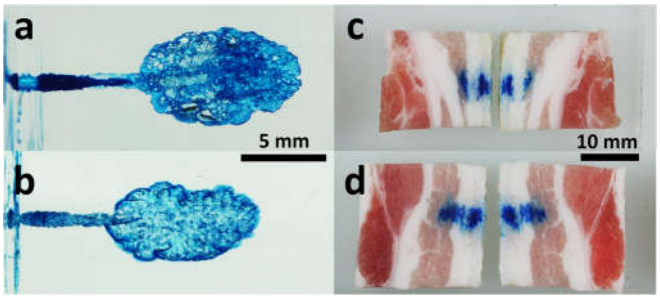

Figure 4. Acrylamide (**left**) and *ex vivo* porcine tissue (**right**) injections of single axial jets produced by the standard nozzle (**top**) and the Injex ampoule (**bottom**).

D. *Radial Jets Nozzle*

High speed imaging of injection using a radial jets nozzle into acrylamide gel shows jet penetration within a couple milliseconds and a fully formed bolus in ~10 ms (Fig. 5a). It is further observed that much of the injected dye escapes through the top side of the bolus at the gel surface. This is because the fracture plane occurs close to the surface of the gel, consequently breaking open the surface, unlike traditional axial jet gel injections. In the image of the acrylamide after injection (Fig. 5b) the two erosion holes curve upwards towards the surface because the acrylamide gel that is previously indented by the spherical end of the nozzle during injection, is restored upwards to its original flat surface post-injection. Injections into porcine tissue (Fig. 5c) yielded injected boluses that remained within the dermis (injection depths of 1.1 and 1.3 mm).

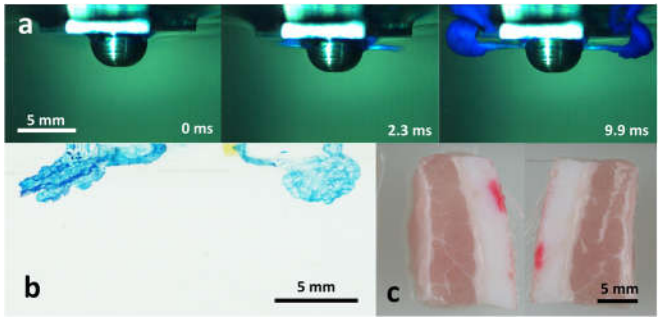

Figure 5. Injections of the radial jets nozzle. (a) High-speed images of an injection into acrylamide gel, (b) image of the erosion holes and boluses in acrylamide gel post-injection, and (c) midline cross section of injected *ex vivo* porcine tissue.

E. *Intersecting Jets Nozzle*

High speed imaging of injection into acrylamide gel using intersecting jets shows the formation of a bolus when the jets intersect (Fig. 6a). The center of the resultant bolus (Fig. 6b) is shallower than that of single axial jets using the same injection parameters (Fig. 4a-b). The two erosion holes are not visible after injection because they are subsumed by the growing fracture plane of the gel during the duration of the injection. When the same jets pierce the tympanic membrane analog, there is insufficient energy to puncture the acrylamide (Fig. 6b) unlike an axial jet produced by an Injex ampoule (Fig. 6c). These results suggest the potential of the intersecting jets nozzle for intratympanic membrane NFI.

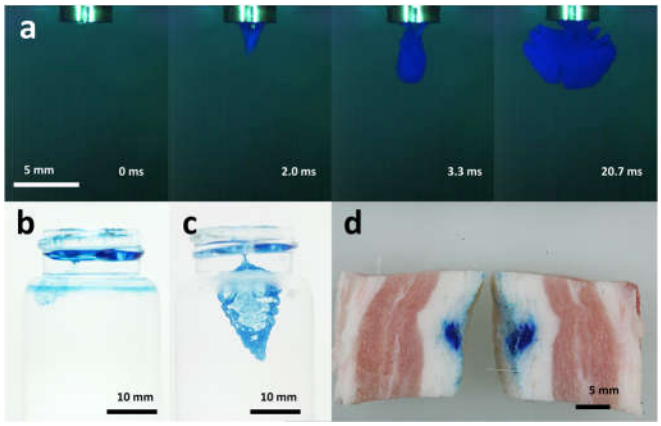

Figure 6. Injections of the intersecting jets nozzle. (a) High-speed images of an injection into acrylamide gel, images of acrylamide gels after tympanic membrane analog injection of (b) the intersecting jets nozzle and (c) the Injex ampoule, and (d) midline cross section of injected *ex vivo* porcine tissue.

E. *Ejection Efficiency*

The ejection efficiencies of the presented configurations range widely between 3% and 19%, with the intersecting jets nozzle exhibiting the highest efficiency and the radial nozzle the lowest efficiency (Fig. 7). Because the power amplifier, controlling electronics, and jet injector are the same,

differences in efficiency should primarily come from the differences of friction between piston and ampoule and fluid flow energy loss in the nozzle orifices. There is no statistical difference between the injection efficiencies using an Injex ampoule or that of a standard nozzle housed in a multi-piece ampoule—both produce single jets of comparable diameter (196 µm and 216 µm, respectively). This similarity may also suggest that the primary ampoule-specific energy loss is due to fluid flow losses and not piston-wall frictional losses, which merits further control studies.

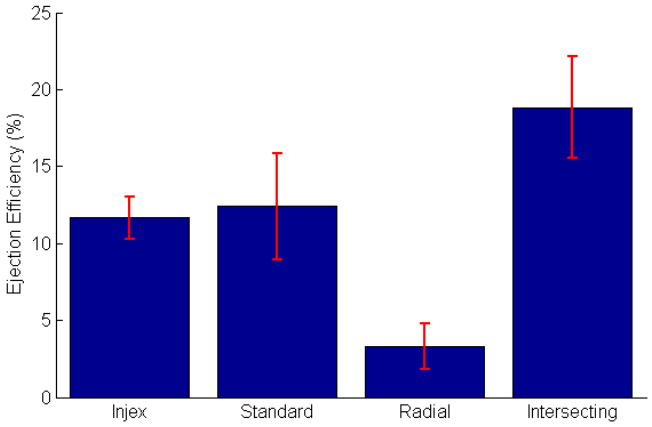

Figure 7. Ejection efficiencies of the studied ampoule configurations. Efficiency is calculated as the ratio between output mechanical kinetic energy of the jet and input electrical energy into the actuator.

We conjecture that the large difference between efficiencies of the nozzles that produce single axial jets and efficiencies of the radial jets and intersecting jets nozzle, are primarily due to head loss in the fluid flow. While the total orifice area of the radial jets nozzle is larger than the standard nozzle and Injex (42.7×10^{-9} m^2 compared to 3.02×10^{-9} m^2 and 0.0366 mm^2, respectively), the diameter—and therefore characteristic length of flow—is up to 20% smaller, leading to a significant decrease in Reynold's number, thereby increasing its nozzle discharge coefficient. The diameter of the orifices of the intersecting jets nozzle (202 µm) are comparable in size with the nozzles that produce single axial jets, however two orifices yield a significantly larger total orifice area (64.1×10^{-9} m^2), thereby decreasing its effective resistance coefficient and decreasing losses. It is also conjectured that slight misalignment between the axes of the piston and ampoule lead to varying frictional losses from trial to trial. Future work will entail improving alignment to decrease variation in ejection efficiency.

V. Conclusion and Future Work

An ampoule platform that houses different nozzle inserts has been developed and demonstrated, enabling a concentration on the design and fabrication of the nozzle geometry instead of the entire ampoule. The ampoule and piston are rigid and therefore increase controllability and the manufacturing process consistently creates nozzles that produce collimated jets and do not deform over time. One nozzle is created to provide comparison with a commercial ampoule, and two other novel geometries are presented and demonstrated to have potential for intradermal and intratympanic membrane injections.

While three-dimensional geometry of the orifice plays a large role in jet creation, the presented work uses orifices of a constant circular cross-section. Future work will entail understanding the effect of 3D orifice geometry on the jet's fluid flow, tissue injection, and efficiency and manufacturing methods to produce various 3D orifice geometries.

Acknowledgment

The authors thank Geehoon Park, a Ph.D. candidate in lab, for assistance in experimental setup and data analysis and Mike Nawrot, a former MS student in lab, for helpful discussions on ampoule design.

References

[1] B.G. Weniger and M.J. Papania, "Alternative vaccine delivery methods (Chapter 61)," in Vaccines, 6th ed. S.A Plotkin, W.A. Orenstein, and P.A. Offit, Eds. Philadelphia: Elsevier/Saunders, 2013, pp. 1200-1231.

[2] J.C. Stachowiak, T.H. Li, A. Arora, S. Mitragotri, and D.A. Fletcher, "Dynamic control of needle-free jet injection," J Control. Release, vol. 135, no. 2, pp. 104-112, January 21, 2009. DOI: 10.1016/j.jconrel.2009.01.003

[3] A.J. Taberner, N.C. Hogan, and I.W. Hunter, "Needle-free jet injection using real-time controlled linear Lorentz-force actuators," Medical Engineering & Physics," vol. 34, no. 9, pp. 1228-1235, November, 2012. DOI: 10.1016/j.medengphy.2011.12.010

[4] A. Modak, N.C. Hogan, and I.W. Hunter, "Adaptive controller for a needle free jet-injector system," oral presentation at *Proc. of 37th Annual International Conference of the IEEE EMBS*, Milan, 2015, pp. 7345-7349. DOI: 10.1109/EMBC.2015.7320088

[5] N.C. Hogan, A.J. Taberner, L.A. Jones, and I.W. Hunter, "Needle-free delivery of macromolecules through the skin using controllable jet injectors," *Expert Opinion Drug Delivery*," vol. 12, no. 10, pp. 1637-1648, May 25, 2015. DOI: 10.1517/17425247.2015.1049531

[6] M.M. Pande S.L. Patwekar, S.G. Gattani. "Needle free injection system: A review," *Int. J. Pharm. Pharm. Sci.*, vol. 5, no. 4, pp. 14–19, 2013. DOI: 10.4103/2230-973X.167662

[7] G. Park, A. Modak, N.C. Hogan, and I.W. Hunter, "The effect of jet shape on jet injection," oral presentation at *Proc. of 37th Annual International Conference of the IEEE EMBS*, Milan, 2015: 7350-7353, DOI: 10.1109/EMBC.2015.7320089

[8] R.M.J. Williams, B.P. Ruddy, N.C. Hogan, I.W. Hunter, P.M.F. Nielsen, and A.J. Taberner, "Analysis of moving-coil actuator jet injectors for viscous fluids," IEEE Transactions on Biomedical Engineering, vol. 63, no. 6, pp. 1099-1106, June 2015. DOI: 10.1109/TBME.2015.2482967

[9] H.D. Ng, R. Portaro, H. Nakayama, "Optimization of drug viscosity used in gas-powered liquid jet injectors". *In Conf. Proc. IEEE Eng. Med. Biol. Soc.* 2015, pages 7354–7357, August 2015. DOI: 10.1109/EMBC.2015.7320090

[10] A.M. Cloutier, "Lorentz-force actuated needle-free injection for intratympanic pharmaceutical delivery," MS Thesis, Department of Mechanical Engineering, MIT, 2013.

[11] A.B. Raynal, N.C. Hogan, and I.W. Hunter, "Design of a debridement device using impinging jets," J. Med. Devices, vol. 10, no. 3, 2016. DOI: 10.1115/1.4033763

[12] B. D. Hemond, A. Taberner, C. Hogan, B. Crane, and I. W. Hunter, "Development and performance of a controllable autoloading needlefree jet injector," Journal of Medical Devices, 2011. DOI: 10.1115/1.4003330

[13] J. Schramm-Baxter, J. Katrencik, and S. Mitragotri, "Jet injection into polyacrylamide gels: investigation of jet injection mechanics," *J Biomech.*, vol. 37, pp. 1181-1188, 2004. DOI: 10.1016/j.jbiomech.2003.12.006